Journal of Membrane Science and Research 5 (2019) 44-48

Journal of Membrane Science & Research

journal homepage: www.msrjournal.com

Research Paper

Optimized Tree-Type Cylindrical-Shaped Nanoporous Filtering Membranes with 6 or 7 Branch Pores in each Pore Tree

Yongbin Zhang*

College of Mechanical Engineering, Changzhou University, Changzhou, Jiangsu Province, China

Article info

Received 2018-07-14
Revised 2018-08-19
Accepted 2018-08-29
Available online 2018-08-29

Keywords

Membrane
Nanopore
Filtration
Separation
Optimization

Highlights

- Novel tree-type cylindrical-shaped nanoporous filtration membranes are proposed.
- The performances of these membranes are investigated.
- The results are instructive to the design and application of these membranes.

Graphical abstract

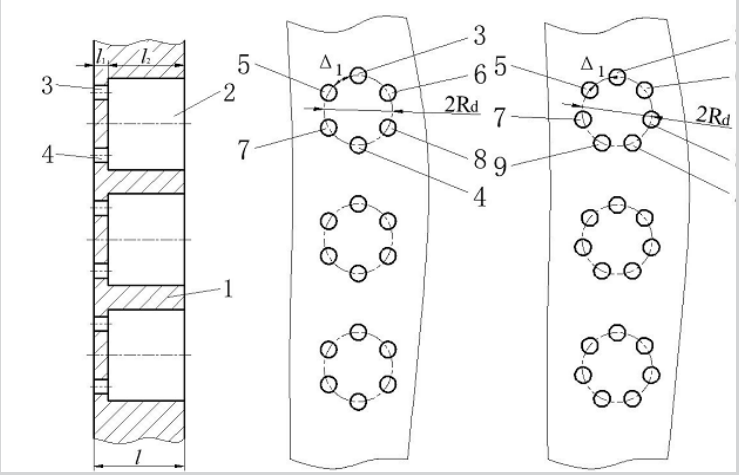

Abstract

The performances of the optimized tree-type cylindrical-shaped nanoporous filtering membranes with six or seven branch pores in each pore tree are analytically studied. The radius $R_{b,1}$ of the branch pore for filtration is normally on the 1 or 10 nm scales. The larger trunk pore is for improving the flux of the membrane. For liquid-particle separations, the radius $R_{b,1}$ of the branch pore is determined by the particle size, and the radius $R_{b,2}$ of the trunk pore is optimized for yielding the lowest flow resistance of the membranes; The optimum ratios of $R_{b,2}$ to $R_{b,1}$ are typically calculated respectively for weak, medium-level and strong liquid-pore wall interactions when the operational parameter values are widely varied. The capability of the liquid-liquid separation of these membranes is also analytically shown.

1. Introduction

Nanoporous filtering membranes have been in fast developments due to their super purification capability [1-6]. One of the challenges to these membranes is that it is not easily reconciled among the filtration capability, flux and mechanical strength of the membranes. People have tried to overcome it by making very thin membranes with the grapheme, taking the filtration pore as conical, or taking the membrane as composed of both nanopores and micropores [7-9].

An optimized cylindrical-shaped nanoporous filtering membrane was proposed in the earlier research [10], across its thickness were distributed respectively two concentric pores with different radii. In this membrane, the smaller pore is for filtration with the nanometer scale radius and pore depth, while the radius of the other larger pore is optimized for yielding the lowest flow resistance of the membrane. Both the flux and the mechanical strength of this membrane are substantially improved.

A tree-type cylindrical-shaped nanoporous filtering membrane was also proposed recently for overcoming the above mentioned challenge [11]. This membrane can be further optimized by taking the branch pore as parallel with its trunk pore and optimizing the radius of the trunk pore for yielding the lowest flow resistance of the membrane [12]. The performance of this membrane is improved with the increase of the number N of the branch pores in each pore tree. However, it was found that the maximum value of N for this membrane is practically around 10 from the viewpoint of engineering application. An over large N cannot result in a more significant reduction of the flow resistance of the membrane, but may cause more difficulty in manufacturing.

In this paper, the performances of the optimized tree-type cylindrical-shaped nanoporous filtering membranes with six or seven branch pores in each pore tree are analytically studied. The optimum ratios of the radius of the trunk pore to the radius of its branch pore and the corresponding lowest dimensionless flow resistances of these membranes are typically calculated respectively for weak, medium-level and strong liquid-pore wall interactions when the operational parameter values are widely varied. For liquid-liquid

* Corresponding author at: Phone: +86 131 96785129; fax: +86 519 86550562
E-mail address: engmech1@sina.com (Y. Zhang)

DOI: 10.22079/JMSR.2018.89954.1203

separations, the optimum values of the radius of the trunk pore in these membranes are calculated for different radii of its branch pore according to the weak liquid-pore wall interaction for widely varying operational parameter values. The liquid-liquid separation capability of these membranes is also investigated. The obtained results are of interest to the design and application of these membranes.

2. Investigated membranes

Figures 1-a-c show the studied tree-type cylindrical-shaped nanoporous filtering membranes with six or seven branch pores in each pore tree. The pore trees are evenly distributed within the membrane. All the branch pores are for filtration and equal with the radius $R_{b,1}$ on the nanometer scale and with the pore depth l_1. The trunk pore has the pore depth l_2 and its radius $R_{b,2}$ is optimized for yielding the lowest flow resistance of the membrane. The branch pore is parallel with its trunk pore. The physical properties of the surfaces of all the pores are identical. The thickness of the membrane is: $l=(l_1+l_2)$.

3. Analysis

The detailed analysis for the studied membranes was presented in Ref. [12]. The necessary contents here are repeated as follows.

In the studied membranes, the N branch pores in each pore tree is equivalent to the straight cylindrical pore with the radius R_{eq}, which is solved from the following equation when neglecting the liquid-pore wall interfacial slippage [12]:

$$\frac{N\cdot Cq(\bar{R}_{b,1})\,|\,S(\bar{R}_{b,1})\,|\,\bar{R}_{b,1}^{4}}{Cy(\bar{R}_{b,1})}-\frac{Cq(\bar{R}_{eq})\,|\,S(\bar{R}_{eq})\,|\,\bar{R}_{eq}^{4}}{Cy(\bar{R}_{eq})}=0 \tag{1}$$

where $\bar{R}_{b,1}=R_{b,1}/R_{cr}$, $\bar{R}_{eq}=R_{eq}/R_{cr}$, R_{cr} is the critical radius of the pore for the passing liquid to become continuum across the pore radius, $Cy(\bar{R})=\eta_{bf}^{eff}(\bar{R})/\eta$, $Cq(\bar{R})=\rho_{bf}^{eff}(\bar{R})/\rho$, ρ_{bf}^{eff} and η_{bf}^{eff} are respectively the average density and the effective viscosity of the passing liquid across the pore radius, S is the parameter describing the non-continuum effect of the passing liquid across the pore radius $(-1\le S<0)$, and ρ and η are respectively the bulk density and the bulk viscosity of the passing liquid at the environmental temperature and pressure.

For a given radius $R_{b,1}$ of the branch pore, increasing the radius $R_{b,2}$ of the trunk pore can reduce the flow resistance of the membrane and thus improve the flux of the membrane. However, an over large $R_{b,2}$ will otherwise increase the flow resistance of the membrane and thus reduce the flux of the membrane, as it significantly reduces the total amounts of the tree-type pores produced on the membrane surface for a given membrane [12]. For yielding the lowest flow resistance of the membrane, there exists the optimum ratio of the radius $R_{b,2}$ of the trunk pore to the radius $R_{b,1}$ of the branch pore which should be calculated as: $(R_{b,2}/R_{b,1})_{opt}=(R_{eq}/R_{b,1})(R_{b,2}/R_{eq})_{opt}$. Here, the optimum ratio of $R_{b,2}$ to R_{eq} is calculated as [12]:

$$\left(\frac{R_{b,2}}{R_{eq}}\right)_{opt}=\begin{cases}\left[\dfrac{(1-\lambda_0)Cq(\bar{R}_{eq})\,|\,S(\bar{R}_{eq})\,|}{\lambda_0 Cy(\bar{R}_{eq})}\right]^{\frac{1}{4}} & ,\ \text{for } R_{b,2}\ge R_{eq}\\ 1 & ,\ \text{for } R_{b,2}<R_{eq}\end{cases} \tag{2}$$

where $\lambda_0=l_1/l$. For a given pressure drop on the membrane and given values of $R_{b,1}$, l_1 and the membrane thickness (l_1+l_2), the value of $R_{b,2}$ calculated from Eq.(2) gives the maximum flux of the membrane if the pressure driven flow occurs within the nanopores of the membrane [12]; Eq.(2) accounts for the effects of the liquid density and viscosity variations and liquid non-continuum property across the radius of the nanoscale branch pore.

For the optimum $R_{b,2}/R_{b,1}$, the corresponding dimensionless lowest flow resistance of the membrane is: $I_{f,\min}=(\bar{R}_r/\bar{R}_{eq})^2F_{\min}$, where $\bar{R}_r=R_r/R_{cr}$, R_r is a constant reference radius, and $F_{\min}$ is [12]:

$$F_{\min}=\begin{cases}2\sqrt{\dfrac{\lambda_0(1-\lambda_0)Cy(\bar{R}_{eq})}{Cq(\bar{R}_{eq})\,|\,S(\bar{R}_{eq})\,|}} & \text{for } R_{b,2}\ge R_{eq}\\ \dfrac{Cy(\bar{R}_{eq})}{Cq(\bar{R}_{eq})\,|\,S(\bar{R}_{eq})\,|} & \text{for } R_{b,2}<R_{eq}\end{cases} \tag{3}$$

In liquid-liquid separations, the optimum value of $R_{b,2}$ should be determined to yield the lowest flow resistance of the membrane for the liquid which has a weak interaction with the pore wall. For the other mixed liquids which may respectively have medium-level or strong interactions with the pore wall, the dimensionless flow resistance of the membrane is: $I_f=(\bar{R}_r/\bar{R}_{eq})^2F(R_{b,2}/R_{eq})$, where $F(R_{b,2}/R_{eq})$ is [12]:

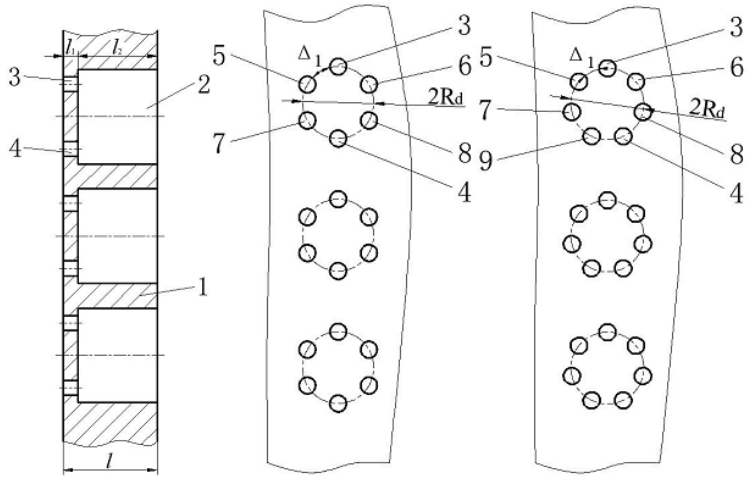

(a) Front view (b) Left-side view, N=6 (c) Left-side view, N=7

1-Membrane substrate; 2-Trunk pore; 3,4,5,6,7,8,9-Branch pores

Fig.1. The optimized tree-type cylindrical-shaped nanoporous filtering membranes with 6 or 7 branch pores in each pore tree studied in the present paper [12].

$$F(\frac{R_{b,2}}{R_{eq}}) = \frac{\lambda_0 Cy(\bar{R}_{eq})}{Cq(\bar{R}_{eq})|S(\bar{R}_{eq})|}(\frac{R_{b,2}}{R_{eq}})^2 + \frac{(1-\lambda_0)Cy(\bar{R}_{b,2})}{Cq(\bar{R}_{b,2})|S(\bar{R}_{b,2})|(\frac{R_{b,2}}{R_{eq}})^2} \quad (4)$$

where $\bar{R}_{b,2} = R_{b,2} / R_{cr}$.

4. Calculation

For the purpose of the liquid-particle separation, the optimum ratios $(R_{b,2} / R_{b,1})_{opt}$ and the corresponding dimensionless lowest flow resistance $I_{f,\min}$ of the membrane were typically calculated respectively for weak, medium-level and strong liquid-pore wall interactions. For the purpose of the liquid-liquid separation, the optimum values of the radius $R_{b,2}$ of the trunk pore were calculated according to the weak liquid-pore wall interaction for varying $R_{b,1}$ and λ_0; For this determined optimum $R_{b,2}$, the dimensionless flow resistances I_f of the membranes were typically calculated for the mixed liquids which may respectively have weak, medium-level and strong interactions with the pore wall, when $R_{b,1}$ varied from 0.5 nm to 20 nm. In the calculations, it was taken that R_r=10 nm.

In the calculations, for whichever liquid-pore wall interaction, $Cq(\bar{R})$ is generally expressed as [12]:

$$Cq(\bar{R}) = \begin{cases} 1 & , \quad \text{for} \quad \bar{R} \geq 1 \\ m_0 + m_1 \bar{R} + m_2 \bar{R}^2 + m_3 \bar{R}^3 & , \text{for } 0 < \bar{R} < 1 \end{cases} \quad (5)$$

where $\bar{R}$ is $\bar{R}_{b,1}$, $\bar{R}_{eq}$ or $\bar{R}_{b,2}$ (same in the following equations), m_0, m_1, m_2 and m_3 are respectively constants.

$Cy(\bar{R})$ is generally expressed as [12]:

$$Cy(\bar{R}) = \begin{cases} 1 & , \quad \text{for} \quad \bar{R} \geq 1 \\ a_0 + \frac{a_1}{\bar{R}} + \frac{a_2}{\bar{R}^2} & , \quad \text{for } 0 < \bar{R} < 1 \end{cases} \quad (6)$$

where a_0, a_1 and a_2 are respectively constants.

$S(\bar{R})$ is generally expressed as [12]:

$$S(\bar{R}) = \begin{cases} -1 & , \quad \text{for} \quad \bar{R} \geq 1 \\ [n_0 + n_1(\bar{R} - n_3)^{n_2}]^{-1} & , \text{for } n_3 < \bar{R} < 1 \end{cases} \quad (7)$$

where n_0, n_1, n_2 and n_3 are respectively constants.

For weak, medium-level and strong liquid-pore wall interactions, the values of R_{cr} were respectively taken as 3.5, 10 and 20 nm [12]. For different types of the liquid-pore wall interaction, the values of the other parameters are respectively shown in Tables 1-a-c.

Table 1-a
Liquid viscosity data for different liquid-pore wall interaction types [12].

Interaction \ Parameter	a_0	a_1	a_2
Strong	1.8335	-1.4252	0.5917
Medium	1.0822	-0.1758	0.0936
Weak	0.9507	0.0492	1.6447E-4

Table 1-b
Liquid density data for different liquid-pore wall interaction types [12].

Interaction \ Parameter	m_0	m_1	m_2	m_3
Strong	1.43	-1.723	2.641	-1.347
Medium	1.30	-1.065	1.336	-0.571
Weak	1.116	-0.328	0.253	-0.041

Table 1-c
Liquid non-continuum property data for different liquid-pore wall interaction types [12].

Interaction \ Parameter	n_0	n_1	n_2	n_3
Strong	0.4	-1.374	-0.534	0.035
Medium	-0.649	-0.343	-0.665	0.035
Weak	-0.1	-0.892	-0.084	0.1

5. Results and discussion

Figure 2-a plots the optimum ratios $(R_{b,2} / R_{b,1})_{opt}$ against the radius $R_{b,1}$ of the branch pore respectively for the weak, medium and strong liquid-pore wall interactions when $\lambda_0 = 1\times10^{-3}$ and N=6 or 7. The value of $(R_{b,2} / R_{b,1})_{opt}$ for N=7 is considerably greater than that for N=6 for the same operating condition, especially when $R_{b,1}$ is relatively big. Figure 2-(b) plots the corresponding dimensionless lowest flow resistances $I_{f,\min}$ of the membranes against $R_{b,1}$ respectively for the weak, medium and strong liquid-pore wall interactions. For the same liquid-pore wall interaction, in Figure 2-b, the curve for N=7 is nearly overlaid with that for N=6. For the same operating condition, it is shown that there is little difference between the resulting lowest flow resistances of the membranes respectively for N=7 and N=6.

Figure 3-a plots the optimum values of the ratio $R_{b,2} / R_{b,1}$ against λ_0 respectively for the weak, medium and strong liquid-pore wall interactions when $\bar{R}_{b,1} = 0.5$ and N=6 or 7. For $\lambda_0 < 1\times10^{-3}$ and the same liquid-pore wall interaction, the optimum value of $R_{b,2} / R_{b,1}$ for N=7 is a bit greater than that for N=6. However, for $\lambda_0 > 1\times10^{-3}$, the differences are further reduced and even minor between the optimum values of $R_{b,2} / R_{b,1}$ respectively for N=7 and N=6 when the liquid-pore wall interactions are the same.

Figure 3-b plots the corresponding dimensionless lowest flow resistance $I_{f,\min}$ of the membranes against λ_0 respectively for the weak, medium and strong liquid-pore wall interactions when $R_r = 10\text{nm}$, $\bar{R}_{b,1} = 0.5$, and N=6 or 7. For a given λ_0 and the same liquid-pore wall interaction, the value of $I_{f,\min}$ for N=7 is a little lower than that for N=6. The value of $I_{f,\min}$ is significantly reduced with the reduction of λ_0 for any N and any liquid-pore wall interaction. Figure 3-b shows that for given λ_0 and N, the value of $I_{f,\min}$ is significantly reduced with the increase of the strength of the interaction between the liquid and the pore wall. This is due to the actually significantly greater values of the dimensional radius $R_{b,1}$ of the branch pore for a stronger liquid-pore wall interaction in the condition of $\bar{R}_{b,1} = 0.5$, as the critical radius R_{cr} is significantly greater for a stronger liquid-pore wall interaction as shown above.

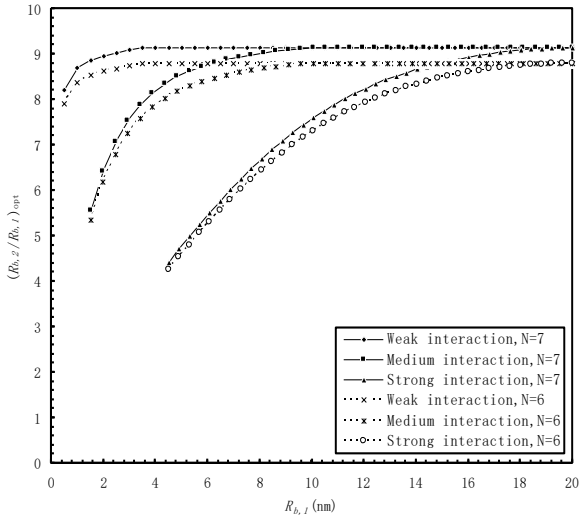

(a)

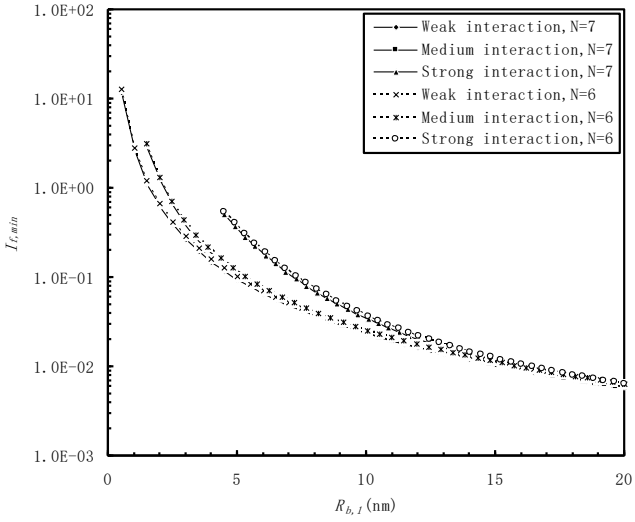

(b)

Fig. 2. Optimum values of the ratio $R_{b,2}/R_{b,1}$ and the corresponding dimensionless lowest flow resistances $I_{f,\min}$ of the membranes respectively for the weak, medium and strong liquid-pore wall interactions when $R_r = 10\text{nm}$, $\lambda_0 = 1\times10^{-3}$, and *N*=6 or 7.

Figure 4 shows the optimum values of the radius $R_{b,2}$ of the trunk pore in the membranes determined according to the weak liquid-pore wall interaction for different $R_{b,1}$ and λ_0. The membranes with these optimum $R_{b,2}$ can be used for liquid-liquid separations when one liquid has a weak interaction with the pore wall while the other liquids have medium or strong interactions with the pore wall.

Figure 5 typically plots the dimensionless flow resistances of the membranes against the radius $R_{b,1}$ of the branch pore for Liquid A, Liquid B and Liquid C, which respectively have the weak, medium and strong interactions with the pore wall, when the radius $R_{b,2}$ of the trunk pore is optimized for achieving the lowest flow resistances of the membranes for Liquid A as shown in Figure 4. The radius $R_{b,1}$ of the branch pore should be no more than 3 nm so that the flow resistance of the membrane for Liquid C, i.e. the strong liquid-pore wall interaction, is more than 10 times that for Liquid A, i.e. the weak liquid-pore wall interaction in the same operating conditions. Further lower values of $R_{b,1}$ give better performances of the membranes in liquid-liquid separations, as the difference between the flow resistances of the membranes for different liquids in the same operating condition is further rapidly increased. There is little difference between the performances of the membranes respectively for *N*=6 and *N*=7 in liquid-liquid separations, as the curves for these membranes in Figure 5 for the same liquids are all overlaid.

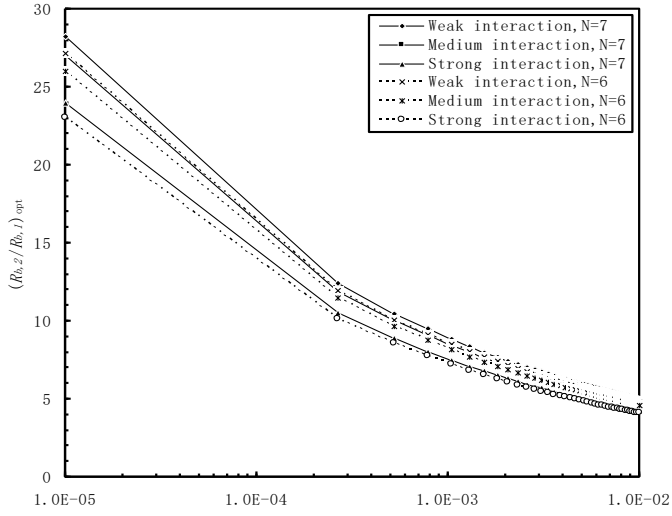

(a)

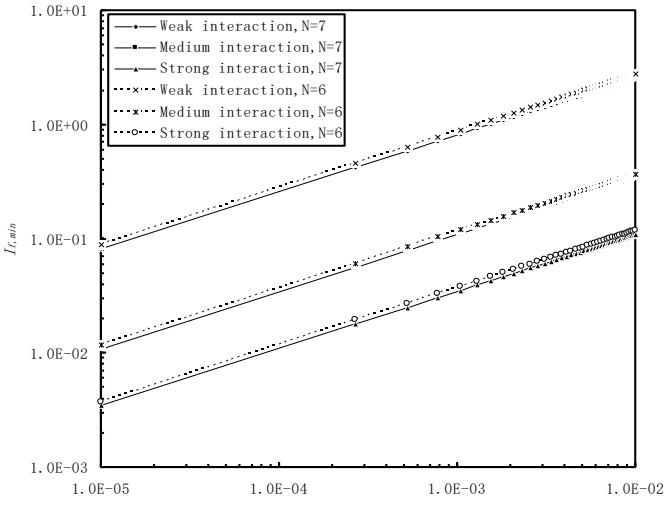

(b)

Fig. 3. Optimum values of the ratio $R_{b,2}/R_{b,1}$ and the corresponding dimensionless lowest flow resistances $I_{f,\min}$ of the membranes respectively for the weak, medium and strong liquid-pore wall interactions when $R_r = 10\text{nm}$, $\bar{R}_{b,1} = 0.5$, and N=6 or 7.

6. Conclusions

The performances of the optimized tree-type cylindrical-shaped nanoporous filtering membranes with the number *N* of the branch pores in each pore tree respectively equal to 6 and 7 are analytically studied. For yielding the lowest flow resistances of these membranes, the optimum ratios of the radius $R_{b,2}$ of the trunk pore to the radius $R_{b,1}$ of the branch pore are typically calculated respectively for the weak, medium and strong liquid-pore wall interactions for $R_{b,1}$ ranging between 0.5 and 20 nm. The corresponding

dimensionless lowest flow resistances of these membranes are also calculated. For the purpose of liquid-liquid separations, the optimum values of $R_{b,2}$ in these membranes are calculated according to the weak liquid-pore wall interaction for widely varying operational parameter values. The performances of the liquid-liquid separations of these membranes are investigated based on the calculated optimum $R_{b,2}$ values. It was found that the liquid-liquid separation capability of these membranes is mainly dependent on both the radius $R_{b,1}$ of the branch pore and the difference among the interactions of the mixed liquids with the pore wall; In the same operating condition, there is little difference between the performances of the membranes respectively for N=6 and N=7 in liquid-liquid separations. The obtained results in this paper are of significant interest to the engineering design and application of the proposed membranes.

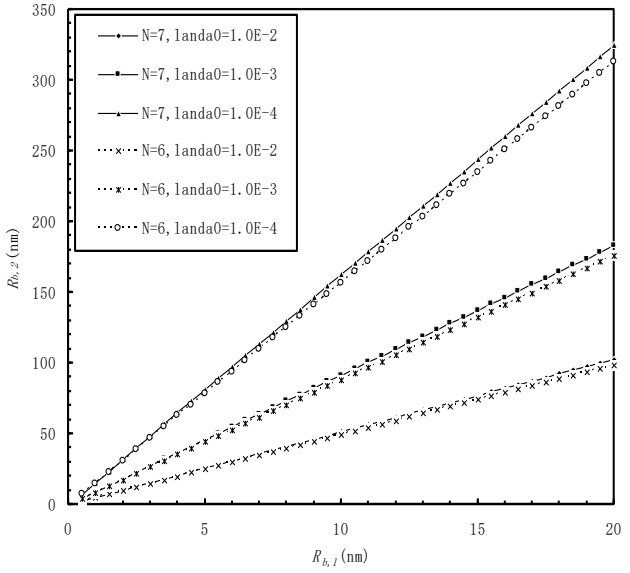

Fig. 4. Optimum values of the radius $R_{b,2}$ of the trunk pore in the membranes determined according to the weak liquid-pore wall interaction.

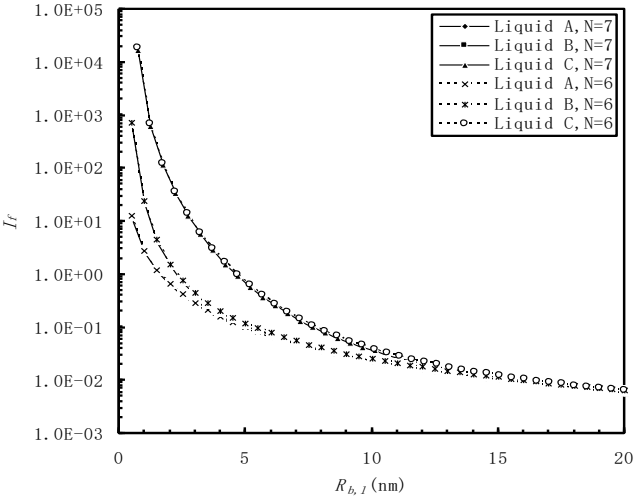

Fig. 5. Plots of the dimensionless flow resistances of the membranes against the radius $R_{b,1}$ of the branch pore respectively for Liquid A, Liquid B and Liquid C when $\lambda_0 = 1\times10^{-3}$ and the radius $R_{b,2}$ of the trunk pore is optimized according to Liquid A as shown in Figure 4.

References

[1] B.J. Hinds, N. Chopra, T. Rantell, R. Andrews, V. Gavalas, L. G. Bachas, Aligned multiwalled carbon nanotube membranes, Science 303 (2004) 62-65.

[2] S.P. Adiga, C. Jin, L.A. Curtiss, N.A. Monteiro-Riviere, R.J. Narayan, Nanoporous membranes for medical and biological applications, Nanomed. Nanobiotech. 1 (2009) 568-581.

[3] J.C. Biffinger, R. Ray, B. Little, B.R. Ringeisen, Diversifying biological fuel cell designs by use of nanoporous filters, Environ. Sci. Technol. 41 (2007) 1444-1449.

[4] W.H. Fissel, A. Dubnisheva, A.N. Eldridge, A.J. Fleischman, A.L. Zydney, S. Roy, High-performance silicon nanopore hemofiltration membranes, J. Membr. Sci. 326 (2009) 58-63.

[5] E.A. Jackson, M.A. Hillmyer, Nanoporous membranes derived from block copolymers: From drug delivery to water filtration, ACS Nano 4 (2010) 3548-3553.

[6] L.A. Baker, S.P. Bird, Nanopores: A makeover for membranes, Nat. Nanotech. 3 (2008) 73-74.

[7] S.P. Surwade, S.N. Smirnov, I.V. Vlassiouk, R.R. Unocic, G.M. Veith, S. Dai, S.M. Mahurin, Water desalination using nanoporous single-layer grapheme, Nat. Nanotechnol. 10 (2015) 459-464.

[8] N. Li, S. Yu, C. Harrell, C.R. Martin, Conical nanopore membranes: Preparation and transport properties, Anal. Chem. 76 (2004) 2025-2030.

[9] S.Y. Yang, I. Ryu, H.Y. Kim, J.K. Kim, S.K. Jang, T.P. Russell, Nanoporous membranes with ultrahigh selectivity and flux for the filtration of viruses, Adv. Mat. 18 (2006) 709-712.

[10] Y.B. Zhang, Optimum design for cylindrical-shaped nanoporous filtration membrane, Int. Commun. Heat Mass Transf. 96 (2018) 130-138.

[11] Y.B. Zhang, A tree-type cylindrical-shaped nanoporous filtering membrane, Front. Heat Mass Transf. 10 (2018) 16.

[12] Y.B. Zhang, An optimized tree-type cylindrical-shaped nanoporous filtering membrane, Front. Heat Mass Transf. 11 (2018) 25.